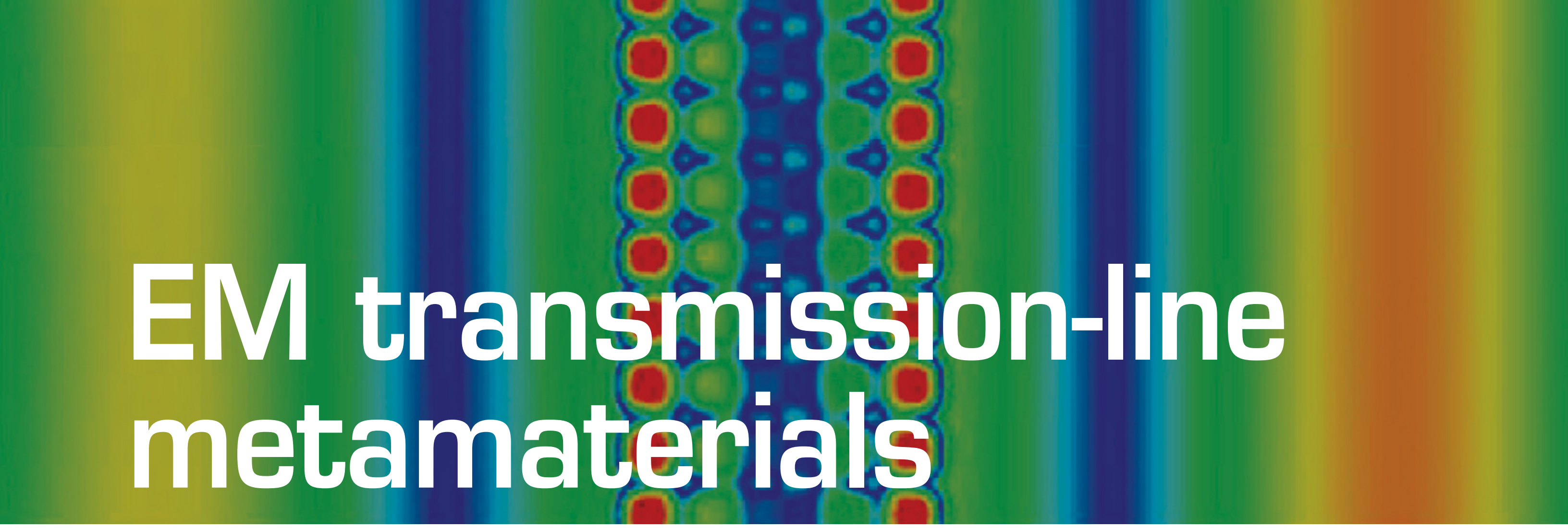

EM transmission-line metamaterials

Metamaterials are understood to be artificially engineered materials that exhibit unusual or difficult to obtain electromagnetic (EM) properties. Such properties would include negative or low values of permittivity, permeability and index of refraction. In this article, we review the fundamentals of metamaterials with emphasis on negative-refractive-index ones, which are synthesized using loaded transmission lines. A number of applications of such metamaterials are discussed, including peculiar lenses that can overcome the diffraction limit and small antennas for emerging wireless communication applications.

George V. Eleftheriades

Department of Electrical and Computer Engineering, University of Toronto, 10 King's College Road, Toronto, ON, M5S 3G4, CANADA

Email: gelefth@waves.utoronto.ca

Artificial dielectrics and metamaterials

Metamaterials are artificially structured media with unusual electromagnetic properties. Typically these are periodic structures consisting of metallo-dielectric scatterers having a periodicity that is much smaller than the impinging and dominant Bloch* wavelengths. In a sense, these constituent scatterers behave like artificial molecules that scatter back an incident electromagnetic wave such that this interaction can be represented using macroscopic effective material parameters such as a permittivity, a permeability and a refractive index. Although the term 'metamaterial' used to describe such structures is relatively new, the basic concept has been around at least since the late 1940s under the name, 'artificial dielectric'.

* *A wave in a periodic structure (1D for clarity) can be described by* $f(x+d) = f(x)e^{-j\beta_{Bloch}d}$ *where d is the periodicity and* β_{Bloch} *is defined as the Bloch propagation constant*[1].

Specifically, at that time, Winston E. Kock of the Bell Telephone Laboratories introduced the concept of the artificial dielectric in order to realize lightweight lenses at microwave frequencies (in the 3-5 GHz range) where the wavelength is long (several centimeters) and thus the corresponding natural dielectric lenses are bulky and heavy[2]. The corresponding 'artificial molecules' were electrically small metallic disks periodically arranged in a concave lens shape. When a plane wave impinges on such an artificial lens with the electric field polarized along the disks, the charges separate on the disks thus creating small dipoles, similar to the molecular dipoles induced in non-polar dielectrics by an impressed field. Kock used simple Lorentz theory to describe his artificial dielectrics summarized by $\varepsilon_{eff} = \varepsilon_0 + N\alpha$, where ε_0 is the permittivity of free space, ε_{eff} is the effective permittivity, N is the number of disks per volume and α is the polarizability of the disks. Using this approach, broadband effective permittivities could

ISSN:1369 7021

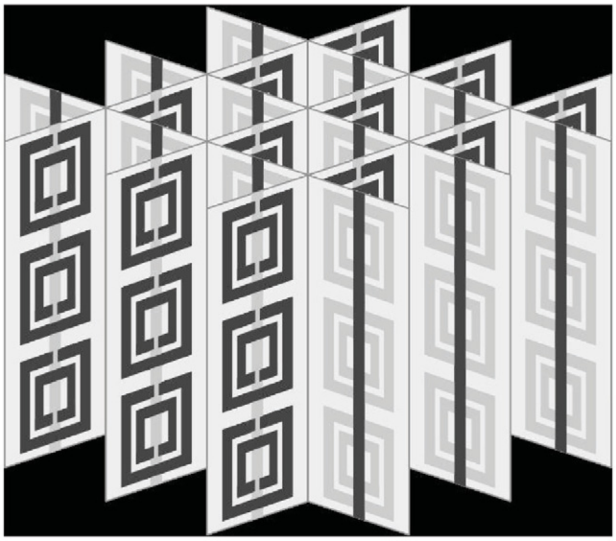

Fig. 1 The split-ring resonator and wire medium. The electric field is polarized along the wires ($\varepsilon < 0$) while the magnetic field permeates the split-ring resonators ($\mu < 0$).

be obtained due to the non-resonant nature of the (small) disks (polarizability fairly constant with frequency). A comprehensive review of artificial dielectrics, including a rigorous mathematical treatment, from that era can be found[3]. Moreover, it is worth mentioning some relevant early work on effective media, including that of Bose who in 1898 used man-made twisted fibers (jute) to rotate the polarization of electromagnetic waves, thus emulating naturally occurring chiral media such as sugar[4]. In a related effort, Lindman in 1914 studied artificial chiral media formed by an ensemble of small wire helices[5].

In this context, metamaterials can be defined as artificial dielectrics but with electromagnetic properties that are inaccessible in nature or are difficult to obtain. Perhaps the most representative metamaterial is the so called 'left-handed' one which is characterized by a simultaneously negative permittivity and permeability, thus implying a negative index of refraction (see Appendix). These hypothetical media were systematically studied by Victor Veselago in the 1960s[6]. To access these unusual material parameters, the constituent unit cells need to be resonant (but still electrically small) which leads to dispersion. Consequently, unlike Kock's artificial dielectrics, metamaterials are usually dispersive in nature.

The split-ring-resonator/wire left-handed metamaterial

In his visionary paper[6], Veselago demonstrated that a hypothetical medium with a negative permittivity and permeability is compatible with Maxwell's equations and went on to describe the electromagnetic properties of such media. For example, he pointed out that in such media the electric field $\bar{E}$, the magnetic field $\bar{H}$ and the propagation vector $\bar{k}$ would follow a left-handed rule (hence the designation 'left-handed' media) and that the phase and group velocities would be anti-parallel (negative index of refraction). However, Veselago did not conclusively prescribe any specific structure that would exhibit these properties. He recognized that plasmas could be used to obtain negative permittivity and he speculated that some kind of a magnetic plasma (not available naturally) would be needed to obtain a negative permeability. The solution to the problem of realizing such a left-handed or negative-refractive-index (NRI) medium was solved three decades later by Shelby, Smith and Schultz[7]. The structure that was used consisted of an array of strip wires to synthesize a negative permittivity and split-ring resonators (capacitively loaded loops) to synthesize negative permeability, as shown in Fig. 1. The use of an array of inductive wires to synthesize artificial dielectrics with plasma-like behavior was previously reported by Walter Rotman[8] (although Rotman never explored the $\varepsilon < 0$ region) and independently by John Pendry[9]. On the other hand, the use of split-ring resonators to synthesize negative permeability media has been suggested by John Pendry[10]. Nevertheless, it should be noted that magnetic particles made of capacitively loaded loops were also suggested by Sergei Schelkunoff in 1952[11] (who was a senior colleague of Winston Kock at Bell Labs at the time). However, Schelkunoff suggested these particles as a means of synthesizing high permeability (and not negative) values but he recognized that such high permeability artificial dielectrics would be quite dispersive.

The negative-refractive-index transmission-line (NRI-TL) metamaterial

An alternative method for realizing 'left-handed' metamaterials consists of loading a host transmission-line medium with reactive elements[12-14]. For example, for synthesizing a left-handed metamaterial in two dimensions, a host microstrip line network can be loaded periodically with series capacitors and shunt inductors as shown in Fig. 2. The key concept is that there is a correspondence between negative permittivity and a shunt inductor (L_0), as well as, between negative permeability and a series capacitor (C_0). This allows one to synthesize artificial media (metamaterials) with a negative permittivity and a negative permeability, and hence a negative refractive index (see Appendix). When the unit cell dimension d is much smaller than the impinging and guided wavelengths, the array can be regarded as a homogeneous, effective medium, and as such can be described by effective constitutive parameters $\varepsilon_{eff}(\omega)$ and $\mu_{eff}(\omega)$ which are determined through a rigorous periodic analysis to be of the form shown in equation 1 (assuming quasi-TEM wave propagation in Fig. 2a)

$$\varepsilon_{eff}(\omega) = 2\varepsilon_p - \frac{g}{\omega^2 L_o d}, \qquad \mu_{eff}(\omega) = \mu_p - \frac{1/g}{\omega^2 C_o d} \tag{1}$$

Here, ε_p and μ_p are positive material parameters describing the filling medium of the host transmission-line and they are proportional to the per-unit-length capacitance C_x and inductance L_x of this host transmission-line medium, respectively (see Fig. 2b). The geometrical

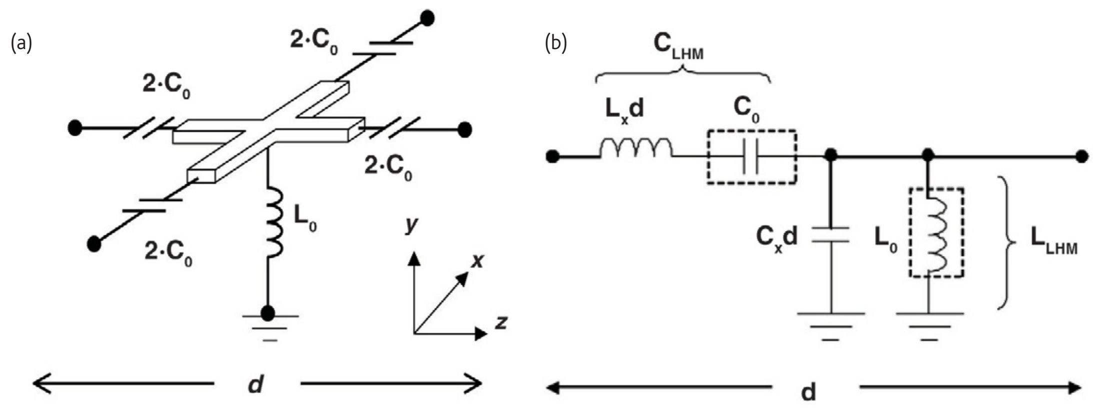

Fig. 2 (a) Unit cell for the 2D NRI-TL metamaterial. A host transmission-line is loaded periodically with series capacitors and shunt inductors. (b) In the limit $\beta d \rightarrow 0$, the interconnecting transmission lines can be replaced by an equivalent series inductance $L_x d$ and shunt capacitance $C_x d$. This yields a "band-pass filter" type of a unit cell which contains both a left-handed and a right-handed response. A modified version of this 1D equivalent circuit can be used to represent axial propagation in the 2D NRI-TL medium (see[12] for the details). Reproduced with permission from the IEEE.

factor g relates the characteristic impedance of the transmission-line network to the wave impedance of the effective medium. Moreover, the factor of two in front of the effective permittivity of the 2D medium is necessary to properly account for scattering at the edges of the unit cell (this factor becomes unity for 1D media).

When inspecting (1) it is seen that as $d \rightarrow 0$, larger and larger values of series capacitors and shunt inductors are needed to maintain a certain index of refraction. This is a practical challenge but not a fundamental one: if the series capacitors are made say using parallel-plates, then as $d \rightarrow 0$, the corresponding C_0 (which is inversely proportional to d) will also increase proportionally thus leaving the product $C_0 d$ constant (a similar argument can be made for the shunt inductors).

A typical dispersion diagram for a 1D negative-refractive-index transmission-line (NRI-TL) medium is shown in Fig. 3. The reader is referred to[15] for the complete 2D dispersion characterization.

As shown in Fig. 3, the lower band is left-handed (backward wave) in which the phase velocity is negative (the wavefronts move toward the source) but the group velocity (slope) is positive (the power moves away from the source). In this lower band, the loading elements C_0, L_0 dominate, whereas at higher frequencies the underlying transmission-line dominates yielding a right-handed (forward-wave) band. Typically, these two bands are separated by a stopband which is delimited by two 'plasma' frequencies f_{c1} and f_{c2}. These are the frequencies at which the effective permittivity $\varepsilon_{eff}(\omega)$ and permeability $\mu_{eff}(\omega)$ vanish, i.e. $\varepsilon_{eff}(\omega) = 0$, $\mu_{eff}(\omega) = 0$. Hence, by setting the effective material

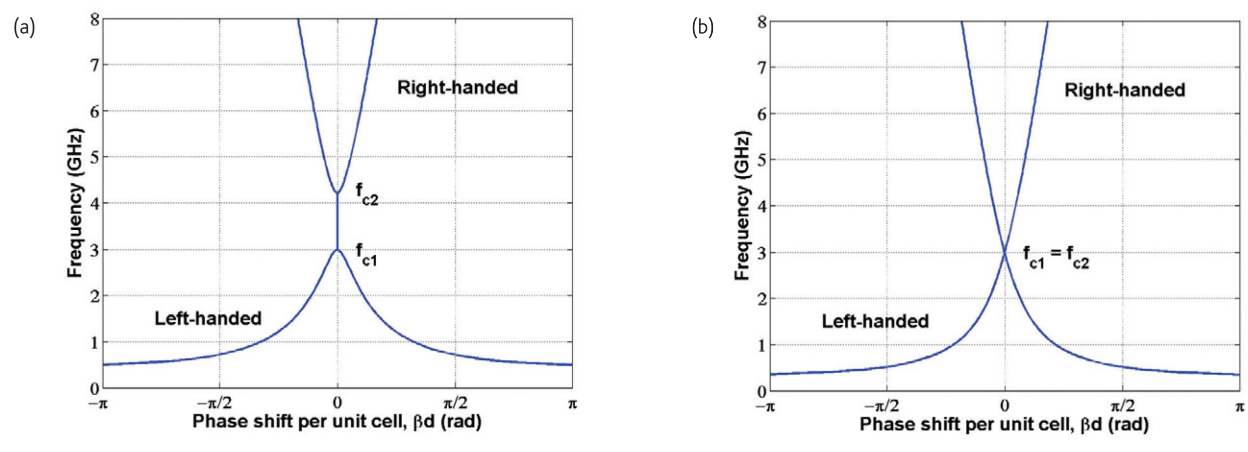

Fig. 3 Sample dispersion diagrams for a one-dimensional NRI-TL (a) Open-stopband case. The interconnecting line is characterized by $\theta = 0.25$rad at 3GHz and $Z_x = 50\ \Omega$ whereas the series loading capacitors are $C_0 = 4.24$pF and the shunt loading inductors are $L_0 = 5.3$nH. The lower band is left-handed (backward wave, negative index) whereas the upper one is right handed (forward wave, positive index). The stopband between these two bands is delimited by the two 'plasma frequencies, f_{c1}, f_{c2}. The size of this stopband is determined by the degree of mismatch between the constituent forward and backward lines: $\frac{f_{c2}}{f_{c1}} = Z_x / \sqrt{L_o / C_o}$.

(b) Closed-stopband case. The interconnecting line is characterized by $\theta = 0.25$rad at 3GHz and $Z_x = 50\ \Omega$ whereas the series loading capacitors are $C_0 = 4.24$ pF and the shunt loading inductors are $L_0 = 10.6$nH such that the closed stopband condition $Z_x = \sqrt{L_0/C_0}$ is satisfied. Note that this case gives access to a zero index of refraction at $f_{c1} = f_{c2} \cong 1/(C_0 Z_x \theta)$ where the artificial medium is matched (nonzero group velocity).

parameters of equation (1) to zero, these cutoff frequencies are readily determined to be,

$$f_{c1} = \frac{1}{2\pi}\sqrt{\frac{1/g}{\mu_p C_o d}} \tag{2}$$

$$f_{c2} = \frac{1}{2\pi}\sqrt{\frac{g}{\varepsilon_p L_o d}} \tag{3}$$

where the characteristic impedance of the host transmission line is $Z_x = g\sqrt{\frac{\mu_p}{\varepsilon_p}} = \sqrt{\frac{L_x}{C_x}}$. By equating f_{c1} and f_{c2}, the stopband in Fig. 3a can be closed thus allowing to access phase shifts around the zero mark, as shown in Fig. 3b (i.e. a zero index of refraction but with the medium still remaining matched). The condition for a closed stopband is therefore determined to be,

$$Z_x = \sqrt{\frac{L_o}{C_o}} \tag{4}$$

This closed stopband condition (4) was derived in[12] (equation 29) and in[13]. Under this condition, the effective propagation constant can be approximated by,

$$\beta_{Bloch} \approx \omega\sqrt{\varepsilon_p \mu_p} - \frac{1}{\omega\sqrt{(L_o d)(C_o d)}} \tag{5}$$

This expression can be interpreted as the sum of the phase incurred by the host transmission line (forward wave) and a uniform backward wave L-C line. Likewise, the corresponding effective index of refraction would be $n = c\beta_{Bloch}/\omega$. Because from (5) there is both a backward (left-handed) and a forward (right-handed) frequency response in the corresponding dominant Bloch propagation constant, in the microwave literature the transmission-line media of Fig. 2 are also known by the name 'Composite-Right-Left-Handed (CRLH)' media.

An electrodynamic point of view

An electrodynamic point of view for interpreting the material parameters for an NRI-TL metamaterial can be obtained by considering the 1D geometry of Fig. 4 which depicts a parallel-plate waveguide loaded by an array of gaps (long slots) and inductive sheets[16].

By applying the Ampère-Maxwell law to the unit cell of the loaded line (over a loop in the x-z plane), the current through the inductive sheets can be represented in terms of a displacement current. In this process, the inductive sheets can be replaced by an equivalent electric polarization given by,

$$\nabla\times\bar{H} = j\omega\varepsilon_0\bar{E} + j\omega\bar{P}_e \text{ where } \bar{P}_e = -\frac{\bar{E}}{\omega^2 L_o d} \tag{6}$$

Likewise, by applying Faraday's law to the unit cell of the loaded line (over a loop in the y-z plane), the voltage drop across the capacitive gaps can be represented in terms of a contribution to the corresponding electromotive force. In this process, the capacitive gaps can be replaced by an equivalent magnetic polarization given by,

$$\nabla\times\bar{E} = -j\omega\mu_0\bar{H} - j\omega\mu_0\bar{P}_m \text{ where } \bar{P}_m = -\frac{\bar{H}}{\mu_o\omega^2 C_o d} \tag{7}$$

The end result is that the loaded parallel-plate waveguide could be represented in terms of an unloaded one but filled with a material having an effective permittivity and permeability given by $\varepsilon_{eff} = \varepsilon_0 - 1/(\omega^2 L_0 d)$, $\mu_{eff} = \mu_0 - 1/(\omega^2 C_0 d)$ respectively.

Discussion of broad bandwidth and low transmission loss

As was mentioned previously, NRI-TL based metamaterials enjoy wide left-handed (backward-wave) passbands and low insertion losses. The origin of these advantages stems from the fact that their constituent C-L resonators are tightly coupled together through their electrical connections. To support this point of view, one can consider the simplest case of an ideal backward line as the limiting case of an array of magnetically coupled loop resonators, as shown in Fig. 5a (in the limit $d \to 2S$)[17].

Using this model, one can show that the dispersion equation for this line of magnetically coupled loop resonators is given by[17],

$$\cos(\beta d) = -\frac{L}{2M_c}\left(1 - \frac{\omega_o^2}{\omega^2}\right) \tag{8}$$

where $\omega_o = 1/\sqrt{LC}$ is the resonant angular frequency of each loop in isolation and $M_c < 0$ is the mutual coupling between adjacent loops

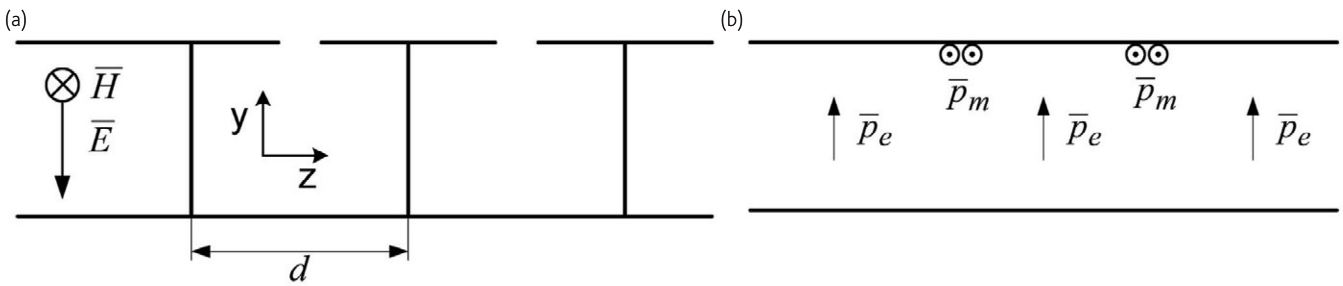

Fig. 4 (a) A 1D parallel-plate waveguide periodically loaded with capacitive gaps and inductive sheets. (b) The equivalent representation of a parallel-plate waveguide in which the inductive sheets and capacitive gaps are represented by equivalent electric and magnetic dipole moments (see text).

(note that a factor of ½ is missing in the definition of M_c in equation 6 of ref.[17]). The limit of electrically connected resonators can be modeled by setting the normalized coupling coefficient $p = -L / 2M_c$ equal to 1 (and in general $1 \leq p < \infty$) as inferred from equation (7) in[17]. A representative set of dispersion diagrams with p as a parameter is shown in Fig. 5b. As shown in Fig. 5b, the tighter the coupling between loops, the wider the backward passband. In other words, the NRI-TL media owe their broad bandwidth to the tight coupling between their constituent C-L loop resonators. Using the above model one can also show that for lossy loop resonators with finite Q, the corresponding insertion loss is minimized when the mutual coupling coefficient M_c is maximum (i.e. when $p \to 1$). These results are not surprising since they form the physical basis for the wide bandwidth and low-loss characteristics of conventional transmission lines.

Connection between SRR/wire and transmission-line metamaterials

The above analysis assumes that the excitation of the transmission-line medium is through some directly attached source. If an array of lines is excited by a plane wave (or one line is embedded in a parallel-plate waveguide) then the situation changes since now the medium will support a forward wave (corresponding to the light line), in addition to the backward wave. The coupling between these two waves will open up a new bandgap (stopband), supporting complex modes, that will reduce the corresponding left-handed bandwidth[18]. The bandwidth can be restored if additional vertical wires are used to bring the forward-wave mode to cutoff[19,20]. This can lead to broadband volumetric (but still 2D) NRI transmission-line media. If these extra wires are offset from the planes of the rings of Fig. 5a then the resulting medium will look very similar to the SRR-resonator/wire medium of Fig.1 but with the SRRs connected[19]. This draws a direct link between left-handed transmission-line and SRR/wire metamaterials and suggests that the bandwidth of the latter can be increased by electrically connecting the SRR at their edges.

Before concluding this subsection it is worth noting that a direct physical 'marriage' between a host planar transmission line and split-ring resonators has been demonstrated thus creating interesting and useful 'hybrid' SRR-loaded transmission-line metamaterial structures[21-22].

Negative refraction

One of the most striking phenomena associated with metamaterials is negative refraction, which is supported by left-handed isotropic metamaterials that are characterized by a negative index of refraction. One way to understand negative refraction is through the notion of phase matching, as explained in Fig. 6. Since Snell's law is a manifestation of phase matching of the transverse propagation vector at the interface between two dielectrics, Fig. 6 readily suggests that the left-handed medium should be characterized by a negative refractive index.

Based on negative refraction a new class of lenses can be envisioned. Examples of such lenses predicted by Veselago are shown in Fig. 7.

When the index is n=-1 the wavelength is equal to that of free space, nevertheless the medium can refract which is somewhat surprising. In fact, this observation can lead to thinner artificial lenses. For example, a plano-convex lens of index n=+2 will be of

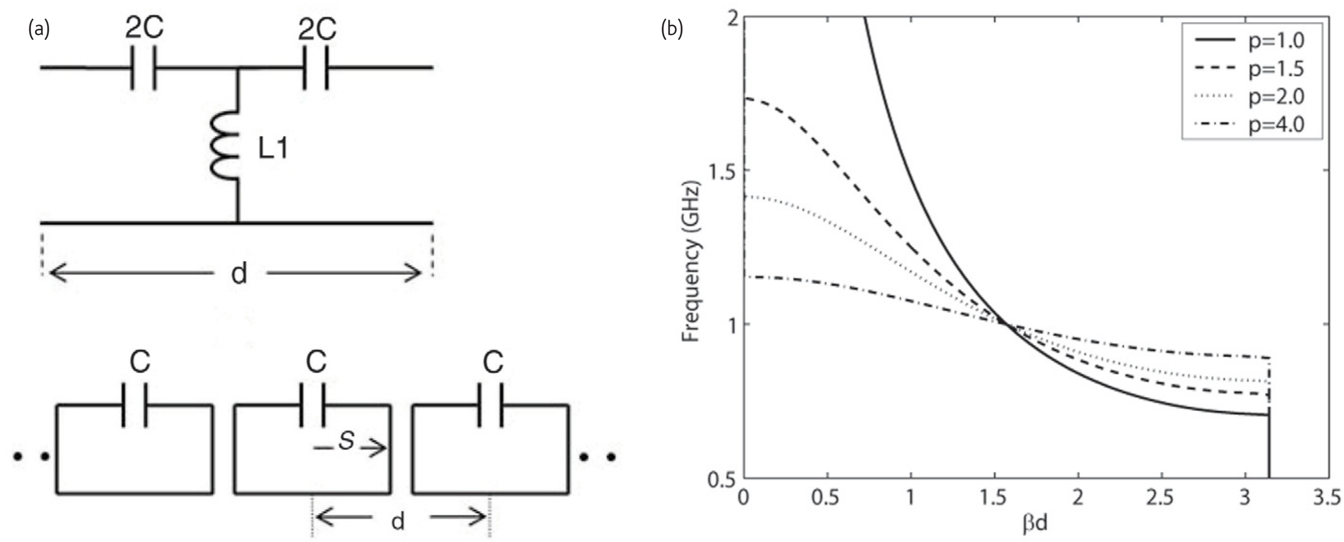

Fig. 5 (a) The unit cell of an ideal backward line and its representation as an array of magnetically coupled loop resonators. The shunt inductance L_1 of the backward line is related to the loop inductance by $2L_1 = L$ (to maintain the same resonant frequency $\omega_o = 1/\sqrt{2L_1C}$). (b)Dispersion diagrams for various normalized mutual coupling coefficients $p = -L / 2M_c$, $\omega_0 = 2\pi\times1GHz$. Maximum coupling occurs by enforcing $p = 1$ which leads to the same dispersion as an ideal backward line for which the bandwidth tends to infinity (note however that infinite bandwidth corresponds to a non-causal solution and it is an idealization. See[17] for the details). Reproduced with permission from IEEE.

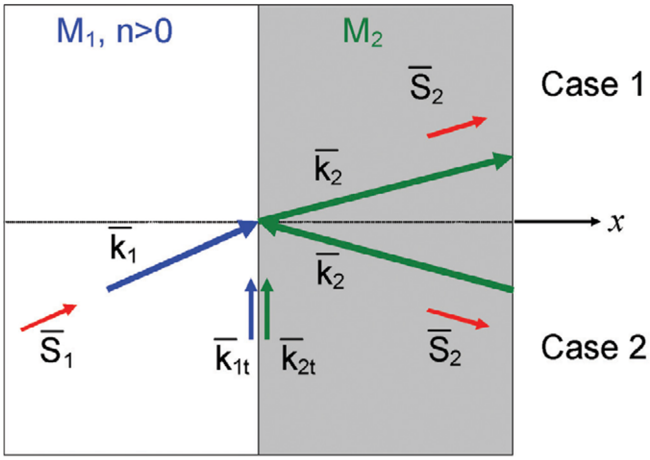

Fig. 6 Negative refraction of a plane wave incident from a regular dielectric to another regular dielectric (Case 1) or a negative-refractive-index medium (Case 2). The arrows on the rays represent the propagation vectors; observe the underlying phase matching of the tangential components of these vectors in Case 2. Another implied principle is that the Poynting Vector S should point away from the interface in the second medium (from[12]). Reproduced with permission from IEEE.

the same power (focal length) as a plano-concave lens of index n=-1. However, the n=+2 lens will have to be twice as thick. Negative index lenses could also offer opportunities in improving lens aberrations (although there will always be a chromatic aberration)[16].

Perhaps the most peculiar negative-index lens is the flat lens without an optical axis which appeared in Veselago's paper[6] and it is shown in Fig.7b.

3D NRI metamaterial structures

Conceptually the 2D SRR/wire medium can be extended to become three dimensional and isotropic by printing a SRR at the six faces of a cubic unit cell and inserting orthogonal wires in *x,y,z* passing through the center of the cube[23]. In a recent related proposal, chiral SRRs (spiral like) are placed on the six faces of a cube to produce a periodic 3D bi-isotropic negative index response[24]. Negative-refractive-index transmission-line metamaterials have also been generalized to three-dimensional isotropic media[25-26]. As was shown in[25], such 3D NRI-TL media can efficiently couple plane waves incident from free space. Figure 8 shows the unit cell for such a 3D isotropic NRI-TL metamaterial. Moreover, this transmission-line approach can be extended to optical frequencies. For this purpose, the key concept arises from the observation that plasmonic (e.g. silver) particles naturally exhibit negative permittivity at optical frequencies and hence can be used to synthesize optical nano-inductors (see equation 1)[27]. Therefore, the unit cell of Fig. 8a can be translated to the optical domain by replacing the inductors with silver particles (e.g. spheres), whereas the capacitors can be obtained through the fringing fields between spheres as suggested in Fig. 8b[28-29]. It could be anticipated that in this transmission-line paradigm, the effect of losses could be minimized, as was discussed previously for the microwave case. Detailed calculations of losses in such optical transmission-line chains of nanoparticles are described[28, 30].

Other concepts for extending NRI-TL metamaterials to three dimensions include the work reported[31]. These are 'scalar' metamaterials in the sense that they cannot interact with arbitrary incident polarization from free space. Instead they are isotropic if

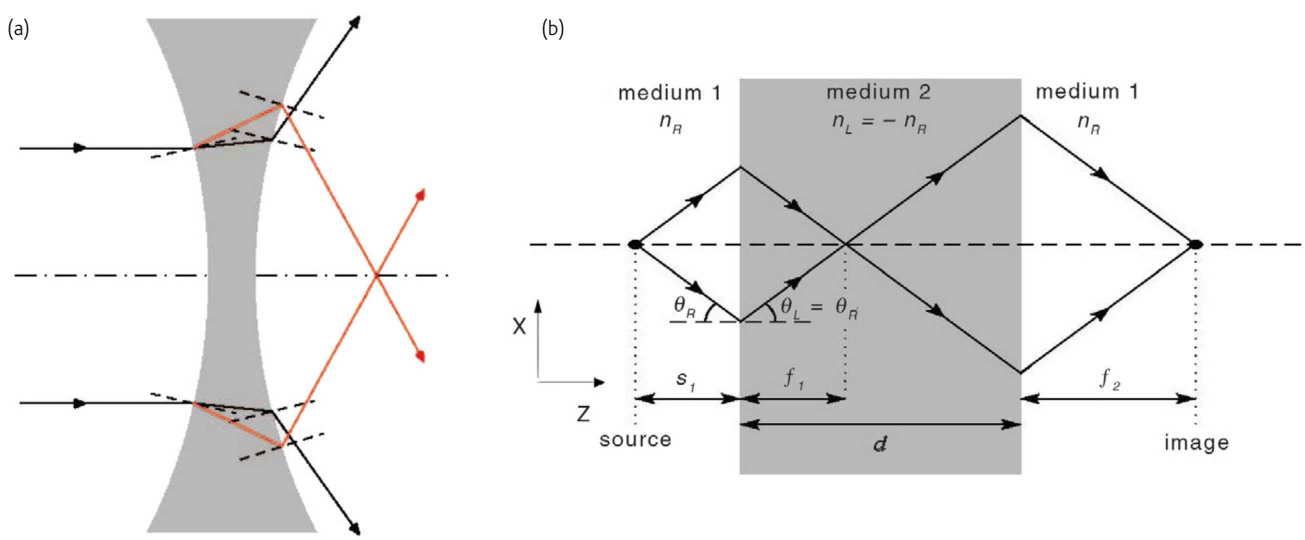

Fig. 7 Peculiar lenses enabled by NRI media (a) A concave lens is diverging for a positive index medium (black line) but converging if the index is negative or less than one (orange line). (b) A Veselago-Pendry lens made out of a slab of a NRI medium. As shown, negative refraction is utilized in order to focus a point to a point. This leads to a lens with flat surfaces and no optical axis. The rays (defined with respect to the Poynting vector, i.e. power flow, in this figure) converge to the same point when the relative index is n=-1 thus leading to aberration-free focusing. The thickness of the lens d is half the distance from the source to the image. (Figures courtesy of Dr Michael Zedler.)

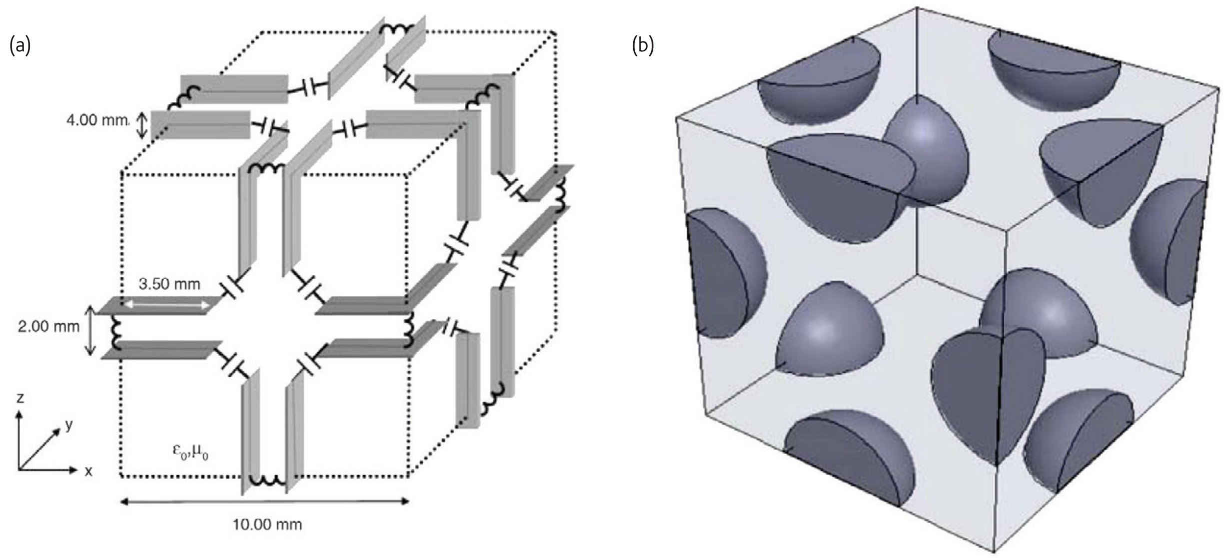

Fig. 8 (a) Unit cell of an isotropic NRI-TL metamaterial for incident plane waves. The unit cell is realizable in broadside coupled-strip-technology and the dimensions shown are for operation in the range 1-1.5 GHz[25]*. Reproduced with the permission from AIP. (b) Unit cell of a possible optical realization of the 3D NRI-TL metamaterial. Optical inductors are realized using closely packed silver spheres (with diameter < 50nm).*

excited with embedded sources such that the pertinent observables are voltages across attached connectors. Another concept for making 3D NRI-TL metamaterials is described[32]. Finally, an interesting structure is based on the so called symmetric condensed node (SCN) that is used to numerically solve Maxwell's equations using the transmission-line matrix (TLM) method[33].

Recently there has been a lot of excitement regarding the implementation of volumetric metamaterials in the optical domain[34-35]. These advances are significant because they show that artificial materials with tailored optical properties could be engineered at the nanoscale. However, there is still much to be done. For example, the metamaterial reported[34] is based on the 'fishnet' structure which can refract the propagation vector negatively but not the Poynting vector (power). On the other hand, the structure of[35] refracts negatively the power by virtue of its anisotropy (a phenomenon similar to the super-prism effect) but not the propagation vector. That is, in both structures negative refraction is caused by anisotropy.

The Veselago-Pendry superlens

One of the most exciting propositions in metamaterial research has been imaging beyond the diffraction limit. This excitement was stirred when John Pendry proposed that the Veselago lens of Fig. 7b could be considered to act as a 'perfect lens'[36]. This proposition should be understood in the context of operating the Veselago lens as a microscope. In this setting, what limits the resolution is the lost transverse wavevectors k_x (assuming 2D propagation for simplicity). The propagating waves $k_x < k_0$ corresponding to large propagation angles with the optical axis, will not be collected by the lens aperture and will be lost. However, if the diameter of the lens is large enough, all these propagating waves will be collected and focused at the image plane, according to the ray diagram of Fig. 7b. However even in this case, the resolution of a conventional lens would be limited because the evanescent waves $k_x > k_0$ (near field) will not make it to the image plane because of their exponential attenuation with distance. Therefore, at best, the resolution of a conventional lens-microscope will be limited by $2\pi / k_0 = \lambda_0$, i.e. by the wavelength of the electromagnetic wave that is used for imaging.

For the Veselago-Pendry lens, the propagating waves $k_x < k_0$ are perfectly restored at the image plane according to the ray diagram of Fig. 7b. In this case, there is perfect matching (no reflections) for all k_x components which is nice given that refraction at oblique incidence on a conventional (positive index) dielectric leads to reflections (even if the dielectric were matched at normal incidence). What is even more surprising though is the fact that the arbitrary evanescent-wave component $k_x > k_0$ is also matched and the corresponding transmission coefficient from the source to the image plane is one (e.g. see pp. 85-87 in[16]). Therefore, at least under ideal conditions the Veselago lens restores a 'perfect' image.

In Fig. 9 the image of a point source (small electric dipole) is plotted through a flatland version of a transmission-line Veselago-Pendry lens[37-38]. Note that the brightest spot lies at the exit interface of the lens and along the line that joins the source and the image. On the other hand, if one inspects the cylindrical wavefronts in Fig. 9a, it becomes apparent that the phase center in each of the three regions identifies the location of the source (leftmost right-handed medium), the center of the NRI-TL slab and the image (rightmost right-handed medium) which is located outside the NRI-TL slab and according to the ray picture of Fig. 9b (despite the fact that this particular lens is only a quarter-wavelength thick, the ray picture seems to remain meaningful, which is somewhat surprising). Therefore in this "super-resolving" mode of operation and around the location of the image a “spot-like” region cannot be identified, since the image region is dominated by the strong evanescent wave components[39]. Nevertheless, this kind of imaging could still be useful, as was demonstrated[40,41] in which a silver film was used as an electrostatic superlens to transfer an optical pattern (mask) from the source plane to the image plane (photoresist) with sub-diffraction resolution.

The fully isotropic 3D structure of Fig. 8a is difficult to realize experimentally. However, by only retaining the horizontal planes of the unit cell shown in Fig. 8a, a volumetric layer-by-layer NRI-TL structure can be easily constructed. The resulting structure will be isotropic for waves having their magnetic fields polarized perpendicularly to the layers. The corresponding structure is shown in Fig. 10 (along with supporting information) and consists of layers of NRI coplanar-strip transmission lines. In order to reduce the losses, high-Q chip capacitors and inductors are used for loading the underlying printed transmission lines[42]. Other recent attempts of superlensing using broadband volumetric and isotropic (but restricted) NRI-TL lenses have been reported[43, 44].

An exciting recent development in the field of the Veselago-Pendry superlens is the magnetic resonance imaging (MRI) application reported in[45]. Specifically, a magnetostatic 3D lens has been constructed, based on the SRR element, that can be used to increase the sensitivity of surface coils. The authors of[45] show a clear improvement of the MRI image of two human knees with and without the presence of the superlens between the knees.

The main drawback of the Veselago-Pendry superlens is that the achieved super-resolution is very sensitive to material losses[46]. A notable example for solving this problem is the so called ‘hyperlens’ which utilizes anisotropic metamaterials that are characterized by a hyperbolic spatial dispersion diagram[47-48]. These hyperbolic media support tightly confined beams (akin to ‘resonance cones’ in anisotropic plasmas) which have been demonstrated earlier at microwaves using transmission-line metamaterials[49]. When these hyperbolic metamaterials are shaped into a cylindrical (or spherical) lens, then the beams that emanate from an object fan out thus magnifying the sub-wavelength features; when they are separated by λ/2 or more, they could be observed using conventional far-field microscopy. Experimental demonstrations of this concept at optical frequencies using layered silver/dielectric structures to synthesize the required hyperbolic metamaterials have been reported in[50-51]. Hyperlenses offer magnification and are significantly less sensitive to material losses but the working distance between the object and the lens must be very small compared to the free-space wavelength .

Finally, it would be interesting to briefly compare imaging using metamaterial superlenses and conventional near-field microscopy. The latter can achieve extreme sub-wavelength resolution but it requires sharp tips and precise mechanical scanning at very close proximity with the specimen. On the other hand, the metamaterial techniques can form the image without scanning (i.e. in parallel, which is attractive for biological imaging), at relaxed distances from the specimen and could offer magnification (e.g. in the case of the hyperlens). Moreover, the parallel imaging formation offered by metamaterial superlenses could prove useful for sub-wavelength photolithography.

Some transmission-line metamaterial antennas

Some of the earliest applications of metamaterials took place at RF/microwave frequencies for the implementation of novel devices such as leaky-wave and small resonant antennas,

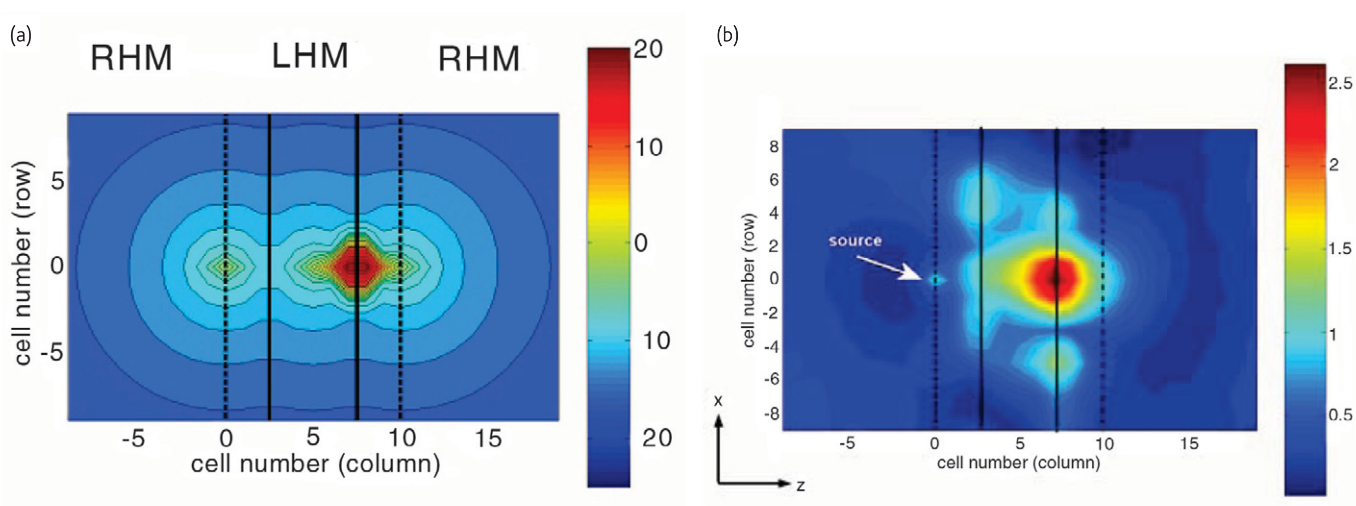

Fig. 9 (a) Calculated vertical electric field just above (in the y-direction) the NRI-TL super-lens[38]. Solid lines designate the NRI-TL boundaries, dotted lines designate the source and image planes. (b) Experimental vertical electric field distribution above a NRI-TL super-lens at 1.057 GHz[37]. Reproduced with the permission from IEEE.

high-coupling level or/and high-directivity couplers, multiband power dividers, small group-delay phase shifters, novel filter architectures etc. Often these devices exploit the peculiar dispersion properties of the backward wave. These properties include the contraction of the guided wavelength as the frequency reduces (which is beneficial for miniaturization) and phase compensation when backward-wave lines are cascaded with natural forward-wave lines (equation 5). These developments are too numerous to describe in detail within a single review article. The reader is referred to some of the books written on metamaterials for this purpose[16, 52-54]. Below we choose to describe a subset of these developments that relate to antenna applications using transmission-line metamaterials.

Leaky-wave antennas

The transmission-line (TL) approach for synthesizing NRI metamaterials has led to the development of new kinds of leaky-wave antennas (LWA). By appropriately choosing the circuit parameters of a several-wavelength long NRI transmission line, a fast-wave structure (i.e. having a phase velocity that exceeds the phase velocity of light in vacuum) can be designed that supports a fundamental spatial harmonic which radiates toward the backward direction[55-57].

Unlike previous work on backward-wave LWAs, which operate in the -1 spatial harmonic[58, 59], these antennas operate in their fundamental spatial harmonic n=0 [1] which facilitates matching and allows for better control of the radiation leakage. Even more interestingly, by enforcing the closed stopband condition of eq (4),

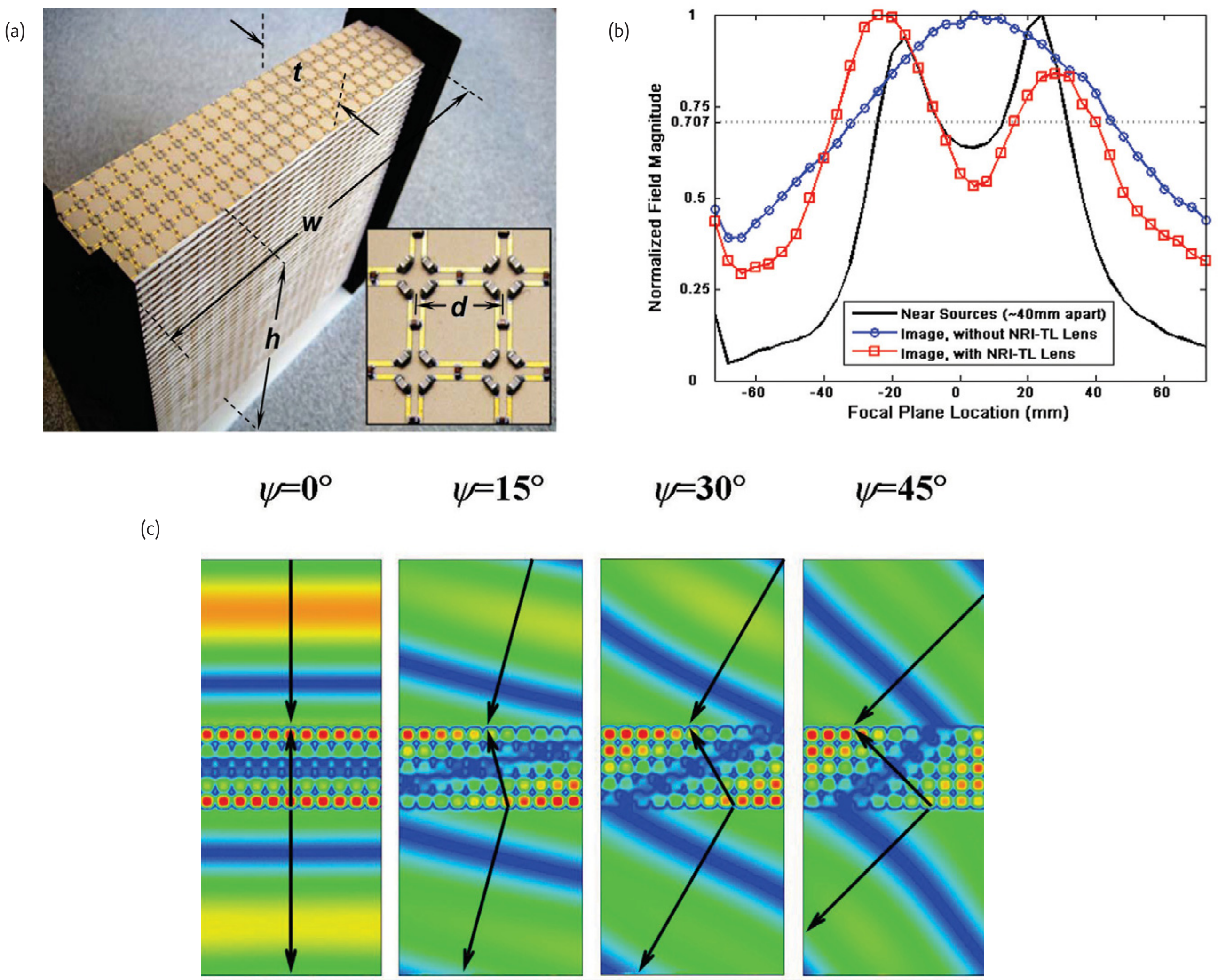

Fig. 10 (a) A free-space Veselago-Pendry NRI-TL superlens. Embedded chip capacitors and inductors are used to minimize losses. The slab consists of 5 x 21cells x 43 layers ($w \times h \times t$ = 150 mm × 150 mm × 35.7 mm, period d = 7 mm). Reproduced with permission from AIP. (b) Super-resolving two sources that are spaced 40mm apart at 2.4 GHz (λ_0 = 125 mm). The sources are magnetic dipoles (small current loops) having their axes perpendicular to the layers of the lens and placed at a distance t/2 = 17.85 mm from the lens. (c) Refraction of a plane-wave obliquely incident on the NRI-TL slab (fullwave simulations). Note the clear demonstration of negative refraction associated with the fundamental spatial harmonic β_{Bloch} (higher spatial harmonics $\beta_n = \beta_{Bloch} + \frac{2\pi n}{d}$, $n = \pm 1, \pm 2, \pm 3, \cdots$ are all present in principle but they are weakly excited).

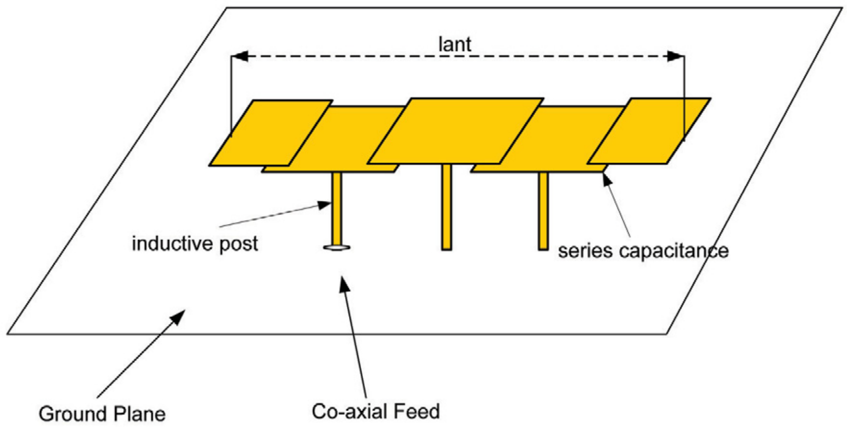

Fig. 11 A miniaturized antenna based on an NRI transmission line. The NRI-TL is implemented using overlapping patches to realize the series capacitance C_0 and attached metallic vias to realize the shunt inductance L_0 (adapted from[62]).

metamaterial transmission-line LWAs can be frequency scanned from the backward (β < 0) to the forward (β > 0) direction through broadside (β = 0), something which was previously thought to be impossible[57,60-61].

NRI-TL small antennas

One method for making small antennas is to exploit the dispersion properties of NRI transmission lines (see equation 5). Specifically, a properly designed NRI transmission line can be made to radiate when its effective electrical length becomes a multiple of half wavelength:

$$\beta_{Bloch} \cdot l_{\text{ant}} = n\pi \text{ where } n = \pm 1, \pm 2, \pm 3 \ldots \tag{9}$$

From (5) it can be inferred that for a given loading L_0, C_0 the effective wavelength $\lambda_{eff} = 2\pi/\beta_{Bloch}$ can be made much shorter than the free-space wavelength. This is especially true at lower frequencies, where the free-space wavelength gets longer, leading to effective antenna miniaturization. A physical realization of such an antenna is shown in Fig. 11 where the NRI transmission line is implemented using overlapping 'mushroom' patches[62]. Typically the length l_{ant} of these antennas can be made quite short (a tenth to a twentieth of a free space wavelength). A useful feature of these antennas is that they can resonate at several frequencies, as implied by eq (9)[62, 63]. Moreover, the mushroom patches can be arranged into 2D patterns for added design flexibility and for dual polarized applications[63]. The main drawback of these NRI-TL antennas though is that they are quite narrowband (typically 1%-2% for a better than 10 dB return loss).

Zero-index small antennas

A related technique for antenna miniaturization consists of operating a short NRI transmission line about the zero-index frequency (where $\beta_{Bloch} = 0$)[64]. The measured return loss of such an antenna having size $\lambda_0/10 \times \lambda_0/10 \times \lambda_0/20$ and operating at 3.1 GHz indicated a 10 dB bandwidth of 53 MHz (1.7%)[65]. The antenna of[65] consisted of 4 unit cells in a 2x2 arrangement. The antenna bandwidth can be increased by detuning the resonance of each constituent unit cell (or groups of unit cells) at a slightly different frequency, thus creating a multi-resonant return-loss passband[66].

Another method for enhancing the bandwidth of the zero-index antenna consists of flattening out the corresponding monopole geometry[67]. In this way, the vias can be made thicker and longer which aids toward increasing the bandwidth. In addition, this approach offers the benefit of reducing the overall height of the antenna. Fig. 12 shows a corresponding single-unit-cell antenna structure which is fed by a co-planar waveguide (CPW) having a truncated ground plane.

To maintain a small size, the antenna consists only of a single unit cell. As shown in Fig. 12b this antenna achieves a very wideband dual-resonance response in a compact and low-profile design. In fact, this is a dual-mode antenna that leads to orthogonal polarizations in the 3.3 – 3.8 GHz WiMax and 5.15 – 5.85 GHz WiFi bands of interest, making it well suited for use in low-cost MIMO systems for wireless LAN applications.

The antenna of Fig. 12a provokes a comment regarding the use of metamaterial concepts for certain applications. Specifically, this antenna was inspired by the concept of a zero-index of refraction. However, the structure only contains a single unit cell and therefore it can be argued that the interpretation of this antenna as a 'metamaterial' one is somewhat farfetched. Nevertheless, this example highlights the point that thinking in terms of the metamaterial paradigm, useful metamaterial-inspired structures can be conceived that only contain very few unit cells. Other interesting and useful examples of small metamaterial-inspired antennas are reported in[68].

Conclusion

The emerging field of metamaterials can be thought of as a rebirth of artificial dielectrics, which formally originated in the 1940s and 1950s, mainly for synthesizing low weight dielectrics for radar applications. However, now, with metamaterials one seeks to synthesize unusual

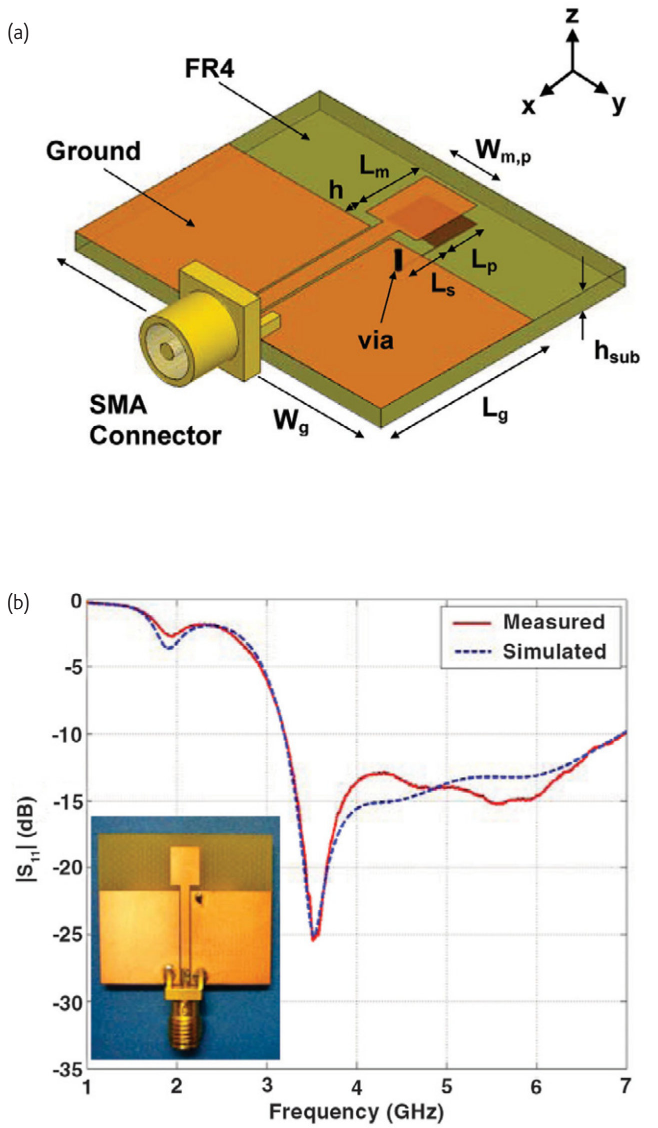

Fig. 12 (a) Layout of the zero-index monopole antenna. All dimensions are in mm: L_m = 6, W_m = 5, L_g = 15, W_g = 30, h = 1, L_p = 4, W_p = 5, L_s = 3.45, W_s = 0.1, h_{sub} = 1.59, S_{cpw} = 0.2, W_{cpw} = 1.55, via diameter = 0.5. Reproduced with the permission from IEEE. (b) The measured and simulated return loss of the zero-index antenna.

electromagnetic properties such as a negative permittivity, a negative permeability, nearly zero or very large values of those, etc. Especially in the optical regime, such concepts have never been applied before and enabled the synthesis of materials with difficult to obtain properties such as a magnetic response[69]. These developments are now becoming meaningful because of substantial improvements in nanofabrication. On the other hand, at microwave frequencies, a new avenue for innovation opened up, leading to novel devices and antennas[16, 52-54].

Finally and with an eye to the future, a very powerful tool for creating with metamaterials has been provided by the visionary papers[70, 71]. These papers describe a method ('transformation optics') for the total control of the electromagnetic field: given a valid distribution of $\bar{B}$ and $\bar{D}$, transformation optics predicts the required material tensors $\bar{\bar{\varepsilon}}(x, y, z)$ and $\bar{\bar{\mu}}(x, y, z)$ to redistribute these field quantities at will. A derived application that captured media attention is (narrowband) cloaking, but we feel that this is only the beginning and many more groundbreaking applications are yet to be discovered[72]. The transformation-optics paradigm highlights a few salient features: metamaterials need not be periodic structures (they can be inhomogeneous) and can be anisotropic. Moreover the control of the fields is achieved in the spatial domain. This brings out an important difference between transmission-line metamaterials and traditional electrical networks and filters (which one may claim that transmission-line metamaterials really are). Unlike electrical networks and filters which primarily control voltage and current quantities in the frequency domain, transmission-line metamaterials should also control the electromagnetic field distribution in the spatial domain (e.g. for designing lenses, cloaks etc.)

Acknowledgement

The author would like to thank Ashwin Iyer for useful interactions and in particular for the discussion of the implications of examining the limit as the periodicity tends to zero in NRI-TL metamaterials. He would also like to thank Marco Antoniades for providing Fig. 12 and for related conceptual contributions. He also thanks Loic Markley and Dr. Michael Zedler.

APPENDIX

Why do negative permittivity and permeability imply a negative index of refraction?

In the lossy case, the material parameters become (assuming a $e^{j\omega t}$ time harmonic variation): $\varepsilon = \varepsilon' - j\varepsilon''$, $\mu = \mu' - j\mu''$, and the index $n = n' - jn''$. For a passive medium the imaginary parts ε'', μ'' and n'' are positive numbers. Now $n = \pm\sqrt{\varepsilon\mu}$ and to choose the right branch of the square root we can use $n^2 = \varepsilon\mu$. Equating the imaginary parts of the latter expression yields $2n'n'' = \varepsilon'\mu'' + \mu'\varepsilon''$ from which it can be inferred that if the real part of the permittivity and the permeability are both negative, i.e. ε' and $\mu' < 0$ then the index of refraction must also be negative, i.e. $n' < 0$. Note that in the main text we are using the relative index defined as the ratio between the speed of light in vacuum to the speed of light in the medium, i.e. the index of refraction is normalized to be $n \to nc$. It is worth noting that this definition for the index of refraction also applies to 1D media (not just 2D or 3D media where refraction can take place).

Group velocity and backward waves

The group velocity is defined as $v_g = \frac{d\omega}{d\beta}$ where $\beta = \omega n/c$ is the propagation constant in the medium. For passive media with Lorentz or Drude dispersion it can be readily shown that the corresponding group velocity is positive. In fact, it can be shown that for passive media the group velocity is always positive; it can only become negative, over narrow bandwidths, around absorption lines (anomalous group velocity) where though the meaning of the group velocity as the velocity of energy transport is lost (e.g. see Mojahedi, M., ***et al.,*** "Abnormal Wave Propagation in Passive Media," IEEE Journal of Selected Topics in Quantum Electronics, Special Issue on Non-Traditional Forms of Light, vol. 9, no 1, pp. 30-39, Jan./Feb. 2003). Therefore in general for negative-refractive-index (NRI) media, the phase velocity is negative (wavefronts move toward the source) whereas the group velocity is positive (power travels away from the source) which implies the propagation of backward waves. mt

REFERENCES

1. Brillouin, L., *Wave Propagation in Periodic Structures,* Dover Publications (2003).
2. Kock, W., *Bell Systems Technical J.* (1948) **27**, 58.
3. Collin, R. E., *Field Theory of Guided Waves*, Piscataway, N.J.: IEEE Press (1990) - chapter 12.
4. Bose, J. C., *Proc. R. Soc.* (1898) **63**, 146.
5. Lindell, I. V., *et al., IEEE Antennas. Propag. Mag.* (1992) **34**, 24.
6. Veselago, V. G., *Soviet Physics Usphekhi* (1968) **10**, 509.
7. Shelby, R. A., *et al., Science* (2001) **292**, 77.
8. Rotman, W., *IRE Transactions Antennas Propag.* (1962) **10**, 82.
9. Pendry, J. B., *et al., Phys. Rev. Lett.* (1996) **76**, 4773.
10. Pendry, J. B., *et al., IEEE Trans. on Microwave Theory and Tech.* (1999) **47**, 2075.
11. Schelkunoff, S. A., and Friis, H. T., *Antennas: Theory and Practice*, John Wiley, New York (1952).
12. Eleftheriades, G. V., *et al., IEEE Trans. on Microwave Theory and Tech.* (2002) **50**, 2702.
13. Sanada, A., *et al., IEEE Trans. Microwave Theory Tech.* (2004) **52**, 1252.
14. Oliner, A. A., A planar negative-refractive-index medium without resonant elements, IEEE Intl. Microwave Symposium Digest, vol. 1, pp. 191-194, Philadelphia, PA, July 2003.
15. Grbic, A., and Eleftheriades, G. V., *IEEE Trans. on Antennas and Propagation* (2003) **51**, 2604.
16. Eleftheriades, G. V., and Balmain, K. G., *Negative-Refraction Metamaterials*, Wiley and IEEE Press (2005).
17. Eleftheriades, G. V., *IEEE Microwave and Wireless Components Lett.* (2007), 412.
18. Elek, F., and Eleftheriades, G. V., *IEEE Microwave and Wireless Components Lett.* (2004) **14**, 434.
19. Rudolph, S. M., and Grbic, A., *IEEE Antennas and Propagation Intl. Symposium* (2007), 2542.
20. Stickel, M., *et al., J. Appl. Phys.* (2007)**102**, 094903.
21. Martín, F., and Bonache, J., *Appl. Phys. Lett.* (2003) **83**, 4652.
22. Falcone, F., *et al., Phys. Rev. Lett.* (2004) **97**, 197401.
23. Koschny, T., *et al., Phys. Rev. B* (2005) **71**, 036617.
24. Jelinek, L., *et al., Phys. Rev. B.* (2008) **77**, 205110.
25. Grbic, A., and Eleftheriades, G. V., *J. Appl. Phys.* (2005) **98**, 043106.
26. Hoefer, W. J. R., *et al.,* Topology and design of wideband 3D metamaterials made of periodically loaded transmission line arrays, in Proc. IEEE Int. Symp. Microwave Theory and Tech., Long Beach, CA, pp. 313-316, June 2005.
27. Engheta, N., *et al., Phys. Rev. Lett.* (2005) **95**, 095504.
28. Alù, A., and Engheta, N., *Phys. Rev. B* (2007) **75**, 024304.
29. Grbic, A., and Eleftheriades, G. V., Plasmonic metamaterials with a negative refractive index, Presented at URSI Radio Science Meeting, Albuquerque, NM, 2006.
30. Alù, A., and Engheta, N., *Phys. Rev. B* (2006) **74**, 205436.
31. Alitalo, P., *et al., J. Appl. Phys.* (2006) **99**, 124910.
32. Zedler, M., *et al., IEEE Trans. Microwave Theory Tech.* (2007) **55**, 2930 and "Systematic Topological Design on Metamaterials: Scalar and Vectrorial 3D Metamaterials and their Realisation," PhD Thesis, Technical University of Munich, 2008, Germany.
33. Iyer, A. K., and Eleftheriades, G. V., *App. Phys. Lett.* (2008) **92**, 261106.
34. Valentine, J., *et al., Nature* (2008) **455**, 376.
35. Yao, J., *et al., Science* (2008) **321**, 930.
36. Pendry, J. B., *Phys. Rev. Lett.* (2000) **85**, 3966.
37. Grbic, A., and Eleftheriades, G. V., *Phys. Rev. Lett.* (2004) **92**, 117403.
38. Grbic, A., and Eleftheriades, G. V., *IEEE Trans. on Microwave Theory and Techniques* (2003) **51**, 2297 (see also Erratum in *IEEE T-MTT* (2004) **52**, 1580).
39. Marqués, R., *et al., Appl. Phys. Lett.* (2006) **89**, 211113.
40. Fang, N., *et al., Science* (2005) **308**, 534.
41. Melville, D. O. S., *et al., Appl. Phys. Lett.* (2004) **84**, 4403.
42. Iyer, A. K., and Eleftheriades, G. V., *Appl. Phys. Lett.* (2008) **92**, 131105.
43. Rudolph, S. M., and Grbic, A., *IEEE Transactions on Antennas and Propagation* (2008) **56**, 2963.
44. Zhu, J., and Eleftheriades, G. V., *Phys. Rev. Lett.* (2008) **101**, 013902.
45. Freire, M. J., *et al., Appl. Phys. Lett.* (2008) **93**, 231108.
46. Smith, D. R., *et al., Appl. Phys. Lett.* (2003) **82**, 1506.
47. Salandrino, A., and Engheta, N., *Phys. Rev. B* (2006) **74**, 075103.
48. Jacob, Z., *et al., Opt. Express* (2006) **14**, 8247.
49. Balmain, K. G., *et al., IEEE Antennas and Wireless Propagation Lett.* (2002) **1**, 146.
50. Smolyaninov, I. I., *et al., Science* (2007) **315**, 1699.
51. Liu, Z., *et al., Science* (2007) **315**, 1686.
52. Engheta, N., and Ziolkowski, R. W., *Electromagnetic Metamaterials: Physics and Engineering Explorations*, Wiley and IEEE Press (2006).
53. Caloz, C., and Itoh, T., *Electromagnetic Metamaterials: Transmission Line Theory and Microwave Applications*, Wiley and IEEE Press (2006).
54. Marqués, R., *et al., Metamaterials with Negative Parameters: Theory, Design and Microwave Applications*, Wiley (2008).
55. Grbic, A., and Eleftheriades, G. V., A backward-wave antenna based on negative refractive index L-C networks, Proc. of the IEEE Intl. Symposium on Antennas and Propagation, San Antonio (2002) Vol. IV, 340.
56. Grbic, A., and Eleftheriades, G. V., *J. Appl. Phys.* (2002) **92**, 5930.
57. Liu, L., *et al., Electronics Lett.* (2002) **38**, 1414.
58. Greiser, J., and Mayes, P., *IEEE Trans. Antennas Propagat.* (1964) **12**, 281.
59. Collin, R. E., and Zucker, F. J., *Antenna Theory - Part II*, McGraw-Hill, New York, (1969).
60. Paulotto, S., *et al., IEEE Trans. Microwave Theory Tech.* (2008) **56**, 2826.
61. Kokkinos, T., *et al., IEEE Trans. on Microwave Theory Tech.* (2006) **54**, 1619.
62. Schussler, M., *et al., IEEE Intl. Microwave Symposium Digest* (2004), 209.
63. Lee, C. J., *et al., IEEE Trans. Antennas and Propagat.* (2006) **54**, 2283.
64. Eleftheriades, G. V., *et al.*, Negative-Refractive-Index metamaterials and enabling electromagnetic applications, Presented at IEEE Intl. Symposium on Antennas and Propagation Digest, Monterey, 2004.
65. Antoniades, M. A., and Eleftheriades, G. V., *IEEE Antennas and Wireless Propagat. Lett.* (2008) **7**, 425.
66. Zhu, J., and Eleftheriades, G. V., *IEEE Antennas and Wireless Propagat. Lett.* (in press).
67. Antoniades, M. A., and Eleftheriades, G. V., *IEEE Antennas and Wireless Propagat. Lett.* (in press).
68. Erentok, A., and Ziolkowski, R. W., *IEEE Trans. on Antenna and Propagat.* (2008) **56**, 691.
69. Linden, S., *et al., IEEE Journal of Selected Topics in Quantum Electronics* (2006) **12**, 1097.
70. Pendry, J. B., *et al., Science* (2006) **312**, 1780.
71. Leonhardt, U., *Science* (2006) **312**, 1777.
72. Shalaev, V. M., *Science* (2008) **322**, 384.